

# Guest Molecular Motion of $[N(CH_3)_4][Cd_3(CN)_7]$ Benzene, Toluene, and Ethylbenzene Clathrates As Studied by $^2H$ NMR

**Shin-ichi Nishikiori\***

*Department of Basic Science, Graduate School of Arts and Sciences, The University of Tokyo, 3-8-1 Komaba, Meguro, Tokyo 153-8902, Japan*

**Takafumi Kitazawa**

*Department of Chemistry, Faculty of Science, Toho University, Funabashi, Chiba 274-8510, Japan*

**Chong-Hyeak Kim**

*Chemical Analysis Laboratory, Korea Research Institute of Chemical Technology, Yusong, Taejeon 305-600, Korea*

**Toschitake Iwamoto**

*Department of Fundamental Science, College of Science and Engineering, Iwaki Meisei University, Chuohdai Iino, Iwaki, Fukushima 970-8551, Japan*

*Received: July 27, 1999; In Final Form: October 29, 1999*

$^2H$  NMR powder patterns of  $[N(CH_3)_4][Cd_3(CN)_7] \cdot nG$  type benzene ( $n = 1.5$ ,  $G = C_6D_6$ ), toluene ( $n = 1$ ,  $G = C_6D_5CD_3$  and  $C_6D_5CH_3$ ), and ethylbenzene ( $n = 1$ ,  $G = C_6D_5CD_2CD_3$ ,  $C_6D_6CH_2CH_3$ , and  $C_6H_5CD_2CH_3$ ) clathrates have been measured between 128 and 468 K and analyzed in order to obtain information about motional behavior of the guest molecules before and during their thermal decomposition. (1) Benzene clathrate: below ca. 300 K the benzene molecule undergoes an ordinary in-plane rotational motion. Above 300 K, a sign of an out-of-plane motion like a precessional motion, which comes from the benzene escaping from the clathrate host owing to its thermal decomposition, was observed. (2) Toluene clathrate: below ca. 320 K the main motion is a  $180^\circ$  flip motion of the aromatic ring and its activation energy is estimated to be 33(1) kJ/mol. Above 320 K, in its thermal decomposition process, an in-plane two-site reorientational motion of the whole toluene molecule takes place. (3) Ethylbenzene clathrate: below ca. 350 K the main motion is a  $180^\circ$  flip motion of the aromatic ring whose activation energy is estimated to be 36(4) kJ/mol, and the ethyl group is undergoing a fast two-site reorientational motion within a restricted space even at 133 K. In a higher temperature region, the reorientational motion of the ethyl group changes to a rotational motion. Detailed motional models for each case have been constructed with several simple motions based on their molecular and crystal structures.

## Introduction

In the course of the remarkable progress of supramolecular chemistry, many chemical compounds with interesting multidimensional framework structures have been generated. A series of polycyano-polycadmates are one of the typical examples of such supramolecular compounds. The multidimensional framework of polycyano-polycadmates is built of cadmium atoms with a tetrahedral or an octahedral coordination structure and cyanides linking two cadmium atoms as a Cd–CN–Cd linkage. A prototype of polycyano-polycadmates had been seen in the Hofmann-type and its related clathrates, which have been known as a typical inclusion compound with cyano metal complex host.<sup>1</sup> However, the discovery of the inclusion ability of cadmium cyanide in 1988<sup>2</sup> was the beginning of the structural development of polycyano-polycadmates, and it has brought a rich harvest so far.<sup>3</sup> In many cases, polycyano-polycadmates form clathrate compounds. The span of the Cd–CN–Cd linkage

is ca. 5.5 Å, and its length is suitable for generating a cavity for small organic molecules in the multidimensional framework structure. So far, many clathrate compounds with a polycyano-polycadmate host have been prepared and investigated by the single-crystal X-ray diffraction method.<sup>3</sup> From these works, much information about the structure of the polycyano-polycadmate hosts has been accumulated. However, few efforts have been made to obtain information about the guest molecules. The clathrate consists of two components: one is the host that has a rigid structure, and another is the guest that is usually in a motional state. The state of the guest has influence on the properties of the clathrate such as guest–guest interaction, guest–host interaction, collaborative phenomena, and so on. The information on the guest is fundamental for clathrate chemistry. X-ray diffraction method is very useful for studying the structures of the host and the guest, but it is not always effective in studying the guest especially in a motional state. From this point of view, we have done some investigations to obtain the information about motional behavior of the guest molecules

\* Author for correspondence. E-mail: cnskor@mail.ecc.u-tokyo.ac.jp. Fax: +81 3 5454 6569.

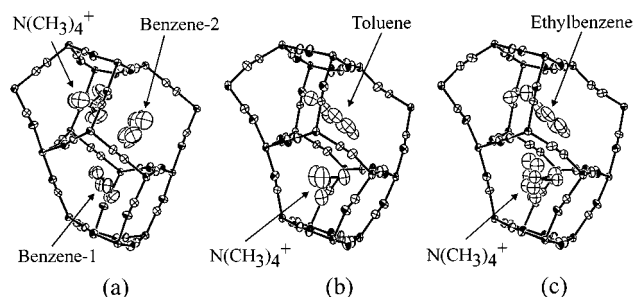


**Figure 1.** Cavity structures of (a) benzene clathrate<sup>6</sup>  $[\text{N}(\text{CH}_3)_4][\text{Cd}_3(\text{CN})_7] \cdot 1.5\text{C}_6\text{H}_6$ , (b) toluene clathrate<sup>6</sup>  $[\text{N}(\text{CH}_3)_4][\text{Cd}_3(\text{CN})_7] \cdot \text{C}_6\text{H}_5\text{CH}_3$ , and (c) ethylbenzene clathrate<sup>7</sup>  $[\text{N}(\text{CH}_3)_4][\text{Cd}_3(\text{CN})_7] \cdot \text{C}_6\text{H}_5\text{CH}_2\text{CH}_3$ .

using solid-state NMR techniques.<sup>4,5</sup> This report is one trial in such works. We have herein tried a <sup>2</sup>H NMR study on clathrates with a polycyano-polycadmate host, in order to obtain systematic information about motional behavior of some different guests trapped in the same cavity. We propose several models of guest molecular motions based on their molecular and crystal structures, and present some pictures about the guest motion in the process of thermal decomposition of the clathrates.

The clathrate that we choose here is  $[\text{N}(\text{CH}_3)_4][\text{Cd}_3(\text{CN})_7] \cdot n\text{G}$ . The composition of the polycyano-polycadmte host is  $[\text{Cd}_3(\text{CN})_7]^-$ , in which two tetrahedral Cd atoms and one octahedral Cd atom are involved in building a three-dimensional framework host structure. To cancel the negative charge of the host, the host includes a tetramethylammonium ion in its inside. And, as a proper guest (G), various small organic molecule can be included in the host framework.<sup>6</sup> The guest species treated in this study are benzene, toluene, and ethylbenzene. The compositions of the clathrates are  $[\text{N}(\text{CH}_3)_4][\text{Cd}_3(\text{CN})_7] \cdot 1.5\text{C}_6\text{H}_6$ ,  $[\text{N}(\text{CH}_3)_4][\text{Cd}_3(\text{CN})_7] \cdot \text{C}_6\text{H}_5\text{CH}_3$ , and  $[\text{N}(\text{CH}_3)_4][\text{Cd}_3(\text{CN})_7] \cdot \text{C}_6\text{H}_5\text{CH}_2\text{CH}_3$ , respectively. Single-crystal X-ray diffraction study<sup>6,7</sup> had already revealed that their hosts are isomorphous. As shown in Figure 1, their cavity structures, which are partial structures of their three-dimensional framework hosts expanding infinitely, are very similar each other.

## Experimental Section

**Preparation.** All samples were prepared according to the method described in our previous papers<sup>6,7</sup> using deuterated guest compounds without purification: benzene  $\text{C}_6\text{D}_6$  (99 atom % D, Aldrich Inc.), toluene  $\text{C}_6\text{D}_5\text{CD}_3$  (99 atom % D, Aldrich Inc.) and  $\text{C}_6\text{D}_5\text{CH}_3$  (99 atom % D, Isotec Inc.), and ethylbenzene  $\text{C}_6\text{D}_5\text{CD}_2\text{CD}_3$  (98 atom % D, Isotec Inc.),  $\text{C}_6\text{D}_5\text{CH}_2\text{CH}_3$  (97 atom % D, Aldrich Inc.), and  $\text{C}_6\text{H}_5\text{CD}_2\text{CH}_3$  (97 atom % D, Isotec Inc.). <sup>2</sup>H NMR powder patterns of the neat deuterated ethylbenzenes measured at 143 K showed that  $\text{C}_6\text{D}_5\text{CH}_2\text{CH}_3$  and  $\text{C}_6\text{H}_5\text{CD}_2\text{CH}_3$  included some isotopic impurities having deuterated methyl group. Their content was estimated from the powder patterns at 143 K. In  $\text{C}_6\text{D}_5\text{CH}_2\text{CH}_3$  the ratio of D atoms in the aromatic part to that in the methyl part was estimated to be 100 to ca. 17; in  $\text{C}_6\text{H}_5\text{CD}_2\text{CH}_3$  the ratio of D atoms in the methylene part to that in the methyl part was estimated to be 100 to ca. 27. These impurities gave us the information about the motional state of the methyl part. All clathrates were obtained as fine crystals and were checked by powder X-ray diffraction method.

**<sup>2</sup>H NMR.** The sample crystals were powdered and packed in a glass tube with a diameter of 5 mm. The tube was sealed with Teflon caps loosely to keep an opening for guest gas released from the sample during its thermal decomposition. <sup>2</sup>H NMR powder patterns were recorded in the temperature range of 128–468 K on a Chemagnetics CMX-300 spectrometer

equipped with a nitrogen gas flow sample temperature controller. The measurement was carried out using the quadrupole pulse sequence<sup>8</sup> with the Larmor frequency of 46.13 MHz, a 90° pulse of 2 μs, interpulse spacing time of 35 μs, and phase alternation. The repetition times were varied between 1 and 30 s to avoid saturation. The observed patterns listed in figures were symmetrized by adding the recorded patterns to its folded ones to improve signal-to-noise ratio. The <sup>2</sup>H NMR line-shape simulation performed in this study is based on the principle described in other several papers.<sup>9</sup> The coordinates setting for describing molecular motional models and computer programs for calculating line shapes in an intermediate motion regime ( $10^4 \text{ s}^{-1} < k$  (jumping rate)  $< 10^7 \text{ s}^{-1}$ ) were the same ones described in our previous papers.<sup>5</sup> For making motional models, we assumed that a sp<sup>3</sup> and a sp<sup>2</sup> carbon atom in the guest molecules had regular tetrahedral and equilateral triangle geometry, respectively. Each observed and simulated powder pattern in figures was normalized to be unit intensity.

**Thermogravimetry.** TG (thermogravimetry) curves of the benzene clathrate  $[\text{N}(\text{CH}_3)_4][\text{Cd}_3(\text{CN})_7] \cdot 1.5\text{C}_6\text{H}_6$ , the toluene clathrate  $[\text{N}(\text{CH}_3)_4][\text{Cd}_3(\text{CN})_7] \cdot \text{C}_6\text{D}_5\text{CD}_3$ , and the ethylbenzene clathrate  $[\text{N}(\text{CH}_3)_4][\text{Cd}_3(\text{CN})_7] \cdot \text{C}_6\text{D}_5\text{CD}_2\text{CD}_3$  were recorded using a Seiko SSC5200 TG/DTA220 thermobalance with ca. 20 mg of the samples and scanning rate of 10 deg min<sup>-1</sup> under air.

## Results and Discussion

**Benzene Clathrate.** In Figure 2 observed <sup>2</sup>H NMR powder patterns of  $[\text{N}(\text{CH}_3)_4][\text{Cd}_3(\text{CN})_7] \cdot 1.5\text{C}_6\text{D}_6$  and simulated patterns are listed. In the temperature range between 133 K and ca. 300 K, the observed patterns were so-called axial patterns in a fast motion regime ( $k > 10^7 \text{ s}^{-1}$ ) with  $Q_{\text{cc}}$  of 92(1) kHz and  $\bar{\eta}$  of 0.00(1). ( $Q_{\text{cc}}$  and  $\eta$  are the quadrupole coupling constant and the asymmetry parameter, respectively.  $Q_{\text{cc}}$  and  $\bar{\eta}$  are motionally averaged ones.) These axial patterns indicate that the benzene guest is undergoing a fast in-plane rotational motion about its 6-fold axis, which is illustrated in Figure 3a as Motion-B1. This in-plane motion of the benzene guest is usually seen at low temperature in many benzene clathrates.<sup>4,5</sup> As shown in Figure 1a, there are two kinds of benzene guests, Benzene-1 and Benzene-2, in the clathrate. However, no sign suggesting a difference between the motional behavior of the two guests was observed in this temperature region.

Between 300 and 350 K, other line shapes were observed. These line shapes had two components: main component was the axial pattern of Motion-B1 observed in the lower temperature region and minor component was a narrower pattern that newly appeared. However, at 353 K the line shape went back to the axial shape. The patterns of Figure 2, e and f, were measured successively at 353 K. Figure 2f showed that the narrower component disappeared during 10 min of the elapsed time of the first measurement of Figure 2e. After the first measurement, the narrower pattern was never observed at any temperature. This finding means that two kinds of motions exist together at first, but one survived and another disappeared rapidly. The former is Motion-B1 and the latter is considered to be an out-of-plane motion because its line width was apparently narrower than that of the axial pattern of Motion-B1. The reason for the disappearance of the narrower pattern is considered to be a release of the benzene guest owing to thermal decomposition of the clathrate. The temperature region where the narrower pattern appears is coincident with the first step of the thermal decomposition of the clathrate. As shown in Figure 4, TG curve showed that the benzene clathrate lost ca. 0.6 of the benzene

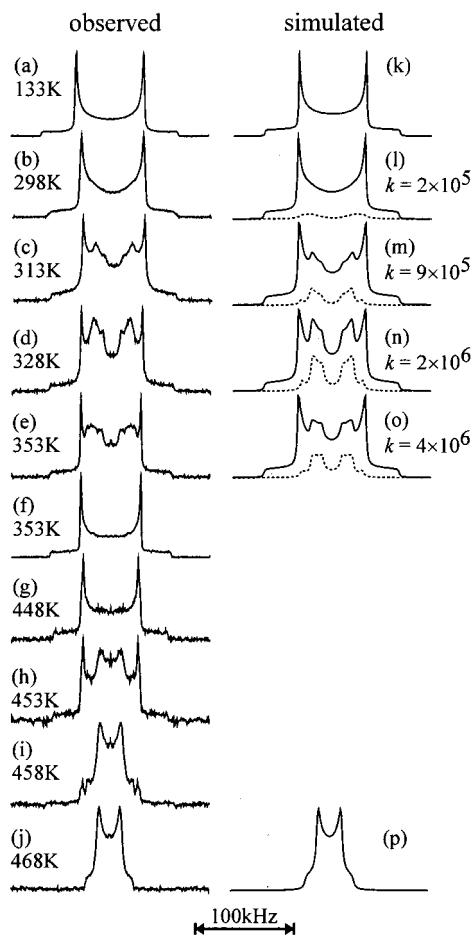


**Figure 2.** (a)–(j) Observed and (k)–(p) simulated <sup>2</sup>H NMR powder patterns of [N(CH<sub>3</sub>)<sub>4</sub>][Cd<sub>3</sub>(CN)<sub>7</sub>]·1.5C<sub>6</sub>D<sub>6</sub>. (k) Simulated pattern based on Motion-B1. (l)–(o) Overlapped figures of two patterns coming from Motion-B1 and Motion-B2. Dashed line is the powder pattern coming from Motion-B2. *k* (s<sup>-1</sup>) is the jumping rate of Motion-B2. (p) Simulated pattern based on Motion-B3.

guest in the temperature range between 300 and 360 K. Therefore, it is considered that the narrower powder pattern reflects the molecular motion of the benzene guest in the thermal decomposition process.

Supplementary information is obtained from the results of our previous X-ray diffraction study at room temperature.<sup>6</sup> The stoichiometry of the benzene guest expected from the crystal structure is 2. However, the actual number of the benzene guest determined from elemental analysis is 1.5.<sup>6</sup> The X-ray diffraction study shows that the occupancies of Benzene-1 and Benzene-2 are respectively 1 and 0.574(4). Although there is a slight disagreement in the guest number derived from the two methods, it is certain that the occupancy of Benzene-2 is about half. This situation is supported from the standpoint of the crystal packing. Each Benzene-1 guest is enclathrated in a separated cavity, so that its full occupancy is possible. On the other hand, Benzene-2 guests are aligned along the *c* axis of the crystal in the host; that is, Benzene-2 is in a tunnel-like cavity along the *c* axis of the crystal. If the occupancy for Benzene-2 is assumed to be 1, the shortest intermolecular distance between carbon atoms of the adjacent Benzene-2 guests is calculated to be 1.75(4) Å. This distance is apparently too short, so that its half-occupancy is quite reasonable. The half-occupancy causes loose packing around Benzene-2 and it gives Benzene-2 space for more vigorous molecular motion such as out-of-plane motion. Such motional state is reflected in the molecular shape derived from the X-ray structure analysis. Benzene-1 is observed as a normal

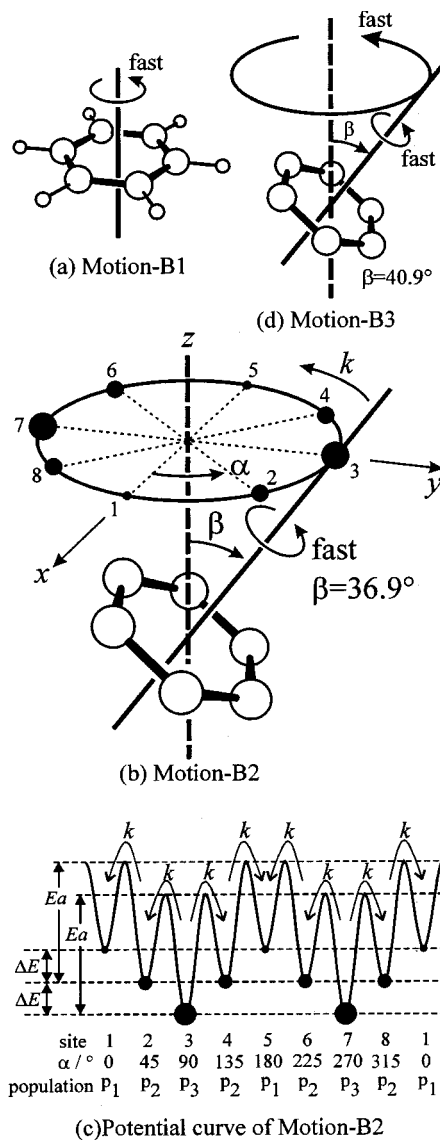


**Figure 3.** (a) Motion-B1. The in-plane rotational motion of Motion-B1 was modeled as a fast six-site reorientational motion where each site was separated by the azimuth ( $\alpha$ ) of 60° and the polar angle ( $\beta$ ) of 90° and the jumping rate (*k*) was 10<sup>8</sup> s<sup>-1</sup>. (b) Motion-B2. A precession-like out-of-plane motion for Benzene-2. The rotation axis is wandering among eight sites whose populations (*p<sub>i</sub>*) are determined according to the mirror symmetry of the crystal. The mirror plane is on the *xz* plane or the *yz* plane. (c) The potential curve of Motion-B2. *k* is the jumping rate from site 2 to site 1 and from site 3 to site 2. *E<sub>a</sub>* is the activation energy of the jump from site 2 to site 1 and that from site 3 to site 2.  $\Delta E$  is the energy difference between site 1 and site 2, and between site 2 and site 3. (d) Motion-B3. A fast precessional motion where the rotation axis is wandering freely on the cone surface of the cone angle  $\beta$ .

planar hexagon with normal thermal factors, and Benzene-2 has a distorted nonplanar shape with large thermal factors. It is natural that the benzene guest in the loose packing and in a vigorous motional state is released at first in the thermal decomposition process. Needless to say, the normal hexagonal shape of Benzene-1 suggests that Benzene-1 has Motion-B1.

On the basis of the above consideration, we present a motional model, Motion-B2, for the narrower pattern of the temperature range between 300 and 350 K. Motion-B2 is illustrated in Figure 3b and its potential curve is shown in Figure 3c. The most considerable out-of-plane motion that appears after the in-plane rotational motion is a precessional motion. However, Benzene-2 is on a mirror plane of the crystal, so that it is assumed that the

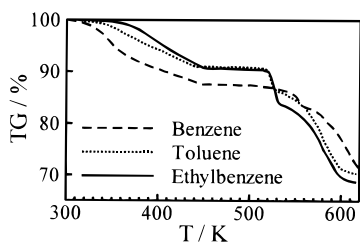


**Figure 4.** TG (thermogravimetry) curves of the benzene clathrate  $[\text{N}(\text{CH}_3)_4][\text{Cd}_3(\text{CN})_7] \cdot 1.5\text{C}_6\text{H}_6$ , the toluene clathrate  $[\text{N}(\text{CH}_3)_4][\text{Cd}_3(\text{CN})_7] \cdot \text{C}_6\text{D}_5\text{CD}_3$ , and the ethylbenzene clathrate  $[\text{N}(\text{CH}_3)_4][\text{Cd}_3(\text{CN})_7] \cdot \text{C}_6\text{D}_5\text{CD}_2\text{CD}_3$ .

rotation axis of this precessional motion undergoes an inequivalent reorientational motion instead of a free rotation in an ordinary precessional motion. We modeled Motion-B2 as an 8-site reorientation of the rotation axis, in which population ( $p_i$ ) of each site was determined to satisfy the mirror symmetry. And we assumed that the jumping rate was common in all jumps between adjacent sites. That is,  $k$  is the jumping rate from site 3 to site 2 and from site 2 to site 1, and  $k'$  is that from site 2 to site 3 and from site 1 to site 2. Then,  $p_3k = p_2k'$  and  $p_2k = p_1k'$  stand from the equilibrium condition. And, if  $p_1$  is considered to be 1,  $p_3$  is calculated to be  $p_2^2$ . Therefore, the line width is determined by two parameters of  $p_2$  and the cone angle  $\beta$  of the precessional motion. There are several value sets of  $p_2$  and  $\beta$  that satisfy the observed line width, but only one combination of  $p_2 = 1.958$  and  $\beta = 36.9^\circ$  showed good agreement with the observed line shapes when the jumping rate ( $k$ ) was scanned in an intermediate motion regime ( $10^4 \text{ s}^{-1} < k < 10^7 \text{ s}^{-1}$ ). On the assumption of the Arrhenius relation and the Boltzmann distribution, the activation energy ( $E_a$ ) and the energy difference between site 1 and site 2 ( $\Delta E$ ) were estimated to be 47(8) kJ/mol and 1.7–2.0 kJ/mol, respectively. The best fit results are shown in Figure 21–o. They are figured as overlapped patterns of Benzene-1 in Motion-B1 and Benzene-2 in Motion-B2.

In the temperature range between 360 and 450 K, observed powder patterns had the axial shape of Motion-B1, and the TG curve showed that ca. 0.5 of the benzene guest was released monotonically. As shown in Figure 2h–j, at ca. 450 K the axial pattern turned rapidly another narrower pattern that seemed to be an axial pattern. Between 450 and 550 K, the TG curve showed a plateau. Apparently, the new narrower axial line shape (Figure 2j) comes from the benzene guest left in the host. This observation is interpreted as follows. The X-ray structure analysis shows that each Benzene-1 is enclathrated in a separated cavity, and the  $^2\text{H}$  NMR powder patterns suggest that each Benzene-1 is undergoing Motion-B1 there. However, the cavity for Benzene-1 is connected to the tunnel cavity for Benzene-2.<sup>6</sup> Therefore, after the first step of the thermal decomposition where Benzene-2 escapes from the tunnel cavity, it becomes possible that Benzene-1 transfers from its own cavity to the tunnel cavity and escapes from the host by way of the tunnel cavity. As the result of this rearrangement and partial release of Benzene-1, space for a more vigorous molecular motion is generated around Benzene-1. It is certain that the structural situation around Benzene-1 was largely changed by the thermal decomposition between 360 and 450 K. The sample once warmed to 468 K did not show the line-shape change observed at ca. 450 K. That sample showed the axial pattern of Motion-B1 below ca. 390 K and showed the narrower axial pattern above ca. 390 K.

The line-shape change at ca. 450 K took place rapidly as an overlap of two line shapes in fast motion regime in a narrow temperature region, so that detailed analysis of the new motional

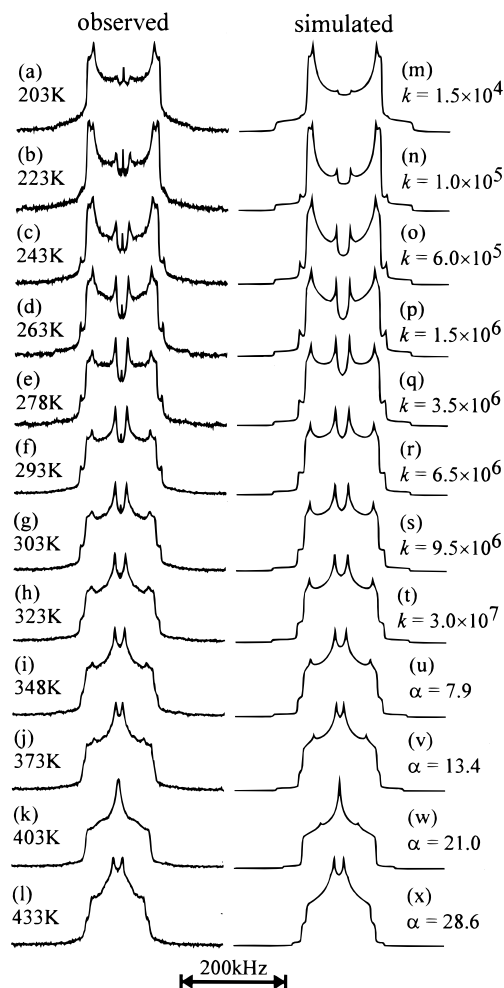


**Figure 5.** (a)–(l) Observed and (m)–(x) simulated  $^2\text{H}$  NMR powder patterns of  $[\text{N}(\text{CH}_3)_4][\text{Cd}_3(\text{CN})_7] \cdot \text{C}_6\text{D}_5\text{CH}_3$ . (m)–(t) Calculated based on Motion-T2.  $k$  ( $\text{s}^{-1}$ ) is the jumping rate of Motion-T2. (u)–(x) Calculated based on Motion-T3 combined with Motion-T2.  $\alpha$  (deg) is the azimuth of Motion-T3.

mode was difficult. In Figure 2p, a simulated pattern based on an ordinary precessional motion (Motion-B3) is shown as a possible model for the motion at 468 K. In Motion-B3, the rotation axis is wandering freely on the cone surface with the cone angle ( $\beta$ ) of  $40.9^\circ$  as shown in Figure 3c. The cone angle value of  $40.9^\circ$  was determined from line-shape simulation.

**Toluene Clathrate.** To obtain detailed information on the molecular motion, we measured  $^2\text{H}$  NMR powder patterns of  $[\text{N}(\text{CH}_3)_4][\text{Cd}_3(\text{CN})_7] \cdot \text{C}_6\text{D}_5\text{CD}_3$  and  $[\text{N}(\text{CH}_3)_4][\text{Cd}_3(\text{CN})_7] \cdot \text{C}_6\text{D}_5\text{CH}_3$ . The observed and simulated patterns are listed in Figures 5 and 6. At 140 K, the line shape of the  $\text{C}_6\text{D}_5\text{CD}_3$  clathrate consists of two patterns (Figure 6a): a wider nonaxial pattern of  $Q_{\text{cc}} = 174(1)$  kHz and  $\eta = 0.078(5)$  coming from the deuterium atoms of the aromatic ring, and a narrower axial pattern of  $Q_{\text{cc}} = 50(1)$  kHz and  $\bar{\eta} = 0.00(2)$  coming from the deuterium atoms of the methyl group. Apparently the methyl group is undergoing fast rotation about its 3-fold axis, which is shown in Figure 7a as Motion-T1. The powder pattern of neat  $\text{C}_6\text{D}_5\text{CD}_3$  observed at 128 K showed  $Q_{\text{cc}} = 181(1)$  kHz and  $\eta = 0.054(5)$  for the aromatic part and  $Q_{\text{cc}} = 52(1)$  kHz and  $\bar{\eta} = 0.00(2)$  for the methyl part. These values were slightly different from those of the toluene guest. Perhaps the toluene guest has a small librational motion. Although details of the libration have been unknown, the libration seems not to include a large anisotropic reorientational mode considering that  $\bar{\eta}$  of



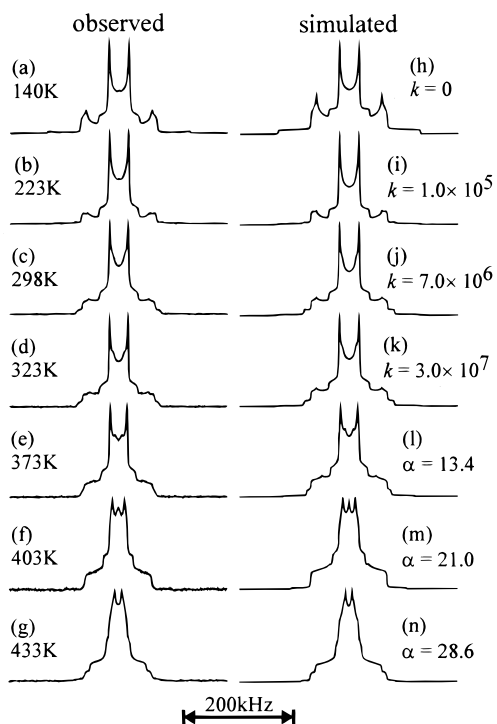


**Figure 6.** (a)–(g) Observed and (h)–(n) simulated <sup>2</sup>H NMR powder patterns for [N(CH<sub>3</sub>)<sub>4</sub>][Cd<sub>3</sub>(CN)<sub>7</sub>]·C<sub>6</sub>D<sub>5</sub>CD<sub>3</sub>. (h)–(k) were calculated based on Motion-T1 and Motion-T2.  $k$  (s<sup>-1</sup>) is the jumping rate of Motion-T2. (l)–(n) were calculated based on Motion-T3 combined with Motion-T1 and Motion-T2.  $\alpha$  (deg) is the azimuth of Motion-T3.

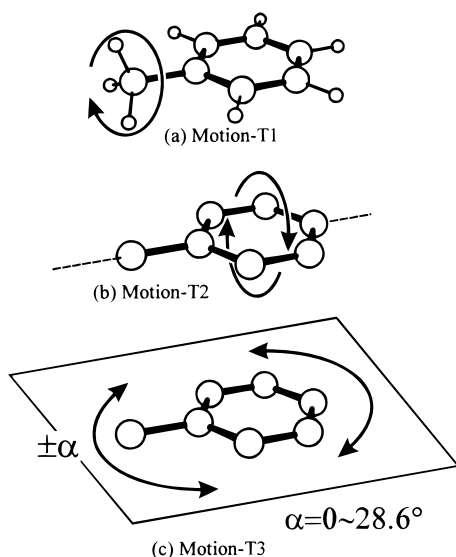


**Figure 7.** (a) Motion-T1. A fast rotational motion of the methyl group was modeled as a three-site reorientation among three sites of  $\alpha = 0, 120, 240^\circ$ ,  $\beta = 70.5^\circ$  with the jumping rate ( $k$ ) of  $10^8$  s<sup>-1</sup>. (b) Motion-T2. A  $180^\circ$  flip motion of the aromatic ring. The motion of D atoms at position 2, 3, 5, and 6 is described as a two-site reorientation between the site with  $\alpha = 0$  and  $\beta = 60^\circ$  and that with  $\alpha = 180^\circ$  and  $\beta = 60^\circ$ . D atom at position 4 has no motion. (c) Motion-T3. An in-plane two-site reorientational motion of the whole toluene guest was modeled as a two-site reorientation between the sites with azimuths of  $\pm\alpha$  with the jumping rate ( $k$ ) of  $10^8$  s<sup>-1</sup>.

the methyl part is maintained to be zero. This small libration was ignored in our line-shape analysis.

A clear change of the line shape of the aromatic part was observed above 220 K in the C<sub>6</sub>D<sub>5</sub>CH<sub>3</sub> clathrate (Figure 5). On the other hand, the line shape of the methyl part was invariant between 140 and 323 K as shown in Figure 6a–d. The X-ray

structure determination shows that the host of the toluene clathrate is similar to that of the benzene clathrate, but the toluene guest has one kind of guest molecule and the toluene guest has a normal molecular shape of a toluene molecule with no distortion and no disorder.<sup>6</sup> Therefore, a possible motion for the aromatic part is a  $180^\circ$  flip motion about the 3-fold axis of the methyl group, which is illustrated in Figure 7b as Motion-T2. The powder patterns simulated based on Motion-T2 are shown in Figure 5m–t. The agreement between the observed and the simulated patterns is quite good. The activation energy for the  $180^\circ$  flip motion of the aromatic ring was derived to be 33(1) kJ/mol on the assumption of the Arrhenius relation.

Above 373 K, the pattern of the methyl part became nonaxial (Figure 6e–g). This finding suggests that a reorientational motion of the whole toluene guest has begun. We here considered an in-plane two-site reorientation for the nonaxial patterns because a part of the line width was maintained over the whole temperature region. Our motional model, Motion-T3, is illustrated in Figure 7c, in which a two-site reorientation takes place on the plane of the aromatic ring. The fast  $180^\circ$  flip motion of the aromatic ring (Motion-T2) is maintained during Motion-T3. Judging from the observed line shapes, Motion-T3 has already reached a fast motion regime at 373 K. The azimuth ( $\alpha$ ) of Motion-T3 at each temperature was determined from the line-shape simulation. The azimuth increases monotonically with a rise in temperature, and reaches  $28.6^\circ$  at 433 K. Figure 5u–x shows the results of the simulation based on Model-T3 combined with Model-T2. Figure 6l–n shows the best fit results of the patterns simulated based of Model-T3 combined with Model-T1 and Model-T2.

The span of a Cd–CN–Cd linkage in the host framework structure is ca. 5.5 Å, so that the wall of the cavity has a hole and one toluene guest contacts with toluene guests in adjacent cavities through the hole. Considering the crystal structure and van der Waals radii, the packing of the toluene guests is not so loose, so that there is not sufficient room for Motion-T3 around the toluene guest.<sup>6</sup> TG curve in Figure 4 showed that a release of the toluene guest began from ca. 300 K and ca. 60% of the guest escaped from the clathrate by 440 K. The decomposition process is coincident with the temperature region of Motion-T3. Therefore, Motion-T3 takes place accompanied by the release of the toluene guests. The sample that had been once heated to 433 K did not show reproducibility of the <sup>2</sup>H NMR line shape. That sample showed a pattern very similar to that at 403 K even at 303 K. The reason for this finding is considered to be the increase of vacancy in the host generated by the release of the toluene guest.

**Ethylbenzene Clathrate.** In the case of the ethylbenzene clathrate, three samples, C<sub>6</sub>D<sub>5</sub>CD<sub>2</sub>CD<sub>3</sub>, C<sub>6</sub>D<sub>5</sub>CH<sub>2</sub>CH<sub>3</sub>, and C<sub>6</sub>H<sub>5</sub>-CD<sub>2</sub>CH<sub>3</sub> clathrate, were prepared and their <sup>2</sup>H NMR powder patterns were measured. The powder patterns of the C<sub>6</sub>D<sub>5</sub>CD<sub>2</sub>-CD<sub>3</sub> clathrate had a large component coming from the ethyl group, especially from the methyl part, so that they were not suitable for examining the aromatic part and the methylene part in detail. In Figures 8 and 9, the powder patterns of the C<sub>6</sub>D<sub>5</sub>-CH<sub>2</sub>CH<sub>3</sub> and the C<sub>6</sub>H<sub>5</sub>CD<sub>2</sub>CH<sub>3</sub> clathrate are shown. Each powder pattern includes the signal from the deuterated methyl group of the impurities as mentioned in the Experimental Section. Line-shape simulation carried out here includes the contribution from the deuterated methyl group.

The line shape of the C<sub>6</sub>D<sub>5</sub>CD<sub>2</sub>CD<sub>3</sub> clathrate at 133 K showed that the large powder pattern coming from the methyl part with  $Q_{cc}$  of 35(1) kHz and  $\bar{\eta}$  of 0.25(3). Apparently, the  $Q_{cc}$  value indicates that the methyl part is undergoing fast rotational motion

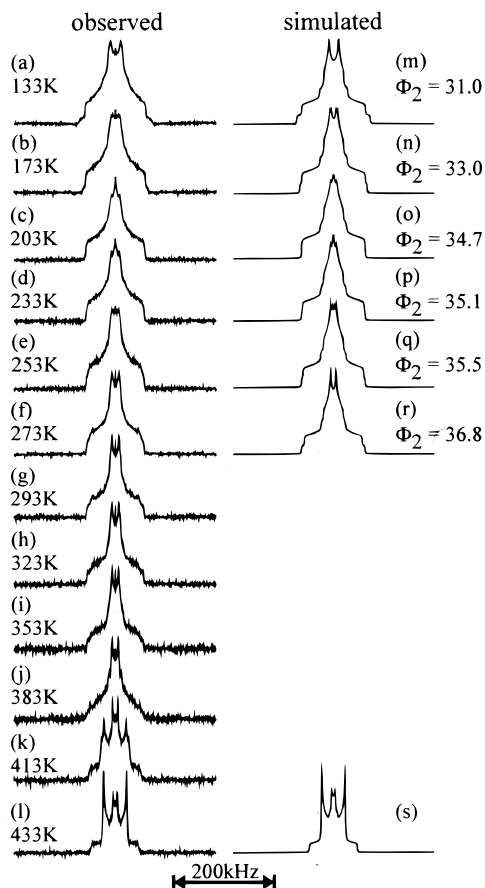


**Figure 8.** (a)–(l) Observed and (m)–(s) simulated  $^2\text{H}$  NMR powder patterns of  $[\text{N}(\text{CH}_3)_4][\text{Cd}_3(\text{CN})_7]\cdot\text{C}_6\text{H}_5\text{CD}_2\text{CH}_3$ . They include the contribution of the  $\text{CD}_3$  group of the impurities. (m)–(r) Calculated based on Motion-E2 combined with Motion-E1.  $\Phi_2$  (deg) is the azimuth of Motion-E2. (s) Calculated based on Motion-E3 combined with Motion-E1.

about its 3-fold axis is shown in Figure 10a as Motion-E1. And Motion-E1 is maintained over the temperature range of this measurement. However, the nonzero  $\bar{\eta}$  shows the existence of another reorientational motion of the 3-fold axis of the methyl group. The powder pattern of the  $\text{C}_6\text{H}_5\text{CD}_2\text{CH}_3$  clathrate at 133 K (Figure 8a) was a line shape in a fast motion regime with  $\bar{\eta}$  of 0.68(1). These observations indicate that the ethyl group is undergoing a fast reorientational motion even at 133 K. However, the pattern of the  $\text{C}_6\text{D}_5\text{CH}_2\text{CH}_3$  clathrate at 133 K (Figure 9a) showed that the aromatic part was almost in a static state. Figure 10c, which is the ethylbenzene guest determined by the single-crystal X-ray structure analysis,<sup>7</sup> shows a large anisotropic thermal ellipsoid of the methylene part. On the other hand, the anisotropy of the methyl part is not large. On the basis of this figure, we considered Motion-E2, which is an in-plane two-site reorientational motion combined with two two-site reorientational motions. One is a two-site reorientation of the whole ethylbenzene between two sites with azimuths of  $\pm\Phi_1$ . Another is a two-site reorientation of the ethyl group between two sites with azimuths of  $\pm\Phi_2$ . As shown in Figure 10b, the guest is jumping between the site with  $-\Phi_1$  and  $+\Phi_2$  and the site with  $+\Phi_1$  and  $-\Phi_2$ . In this motion the aromatic ring is on a plane, and the position of methyl group is almost kept at the same position, but only the methylene part moves largely. These motional situations agree with the guest structure obtained from the X-ray diffraction study. In Figure 8m–r, powder patterns of  $\text{C}_6\text{H}_5\text{CD}_2\text{CH}_3$  simulated based on Motion-E2 are shown. In this simulation,  $\Phi_1$  and  $\Phi_2$  were scanned and we obtained best

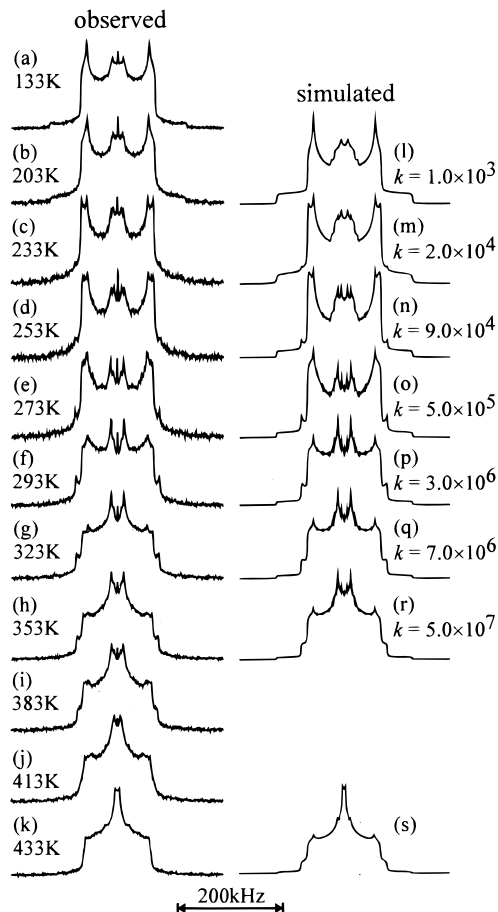


**Figure 9.** (a)–(k) Observed and (l)–(s) simulated  $^2\text{H}$  NMR powder patterns of  $[\text{N}(\text{CH}_3)_4][\text{Cd}_3(\text{CN})_7]\cdot\text{C}_6\text{D}_5\text{CH}_2\text{CH}_3$ . They include the contribution of the  $\text{CD}_3$  group of the impurities. (l)–(r) Calculated based on Motion-E1, Motion-E2, and Motion-E4.  $k$  ( $\text{s}^{-1}$ ) is the jumping rate of Motion-E4. (s) Calculated based on Motion-E1, Motion-E3, and Motion-E4.

fit results under the conditions that  $\Phi_1$  was fixed to  $10^\circ$  at any temperature and  $\Phi_2$  was  $31.0^\circ$ – $36.8^\circ$  depending on temperature. The ethylbenzene is trapped in the cavity in a manner similar to the toluene clathrate, so that random isotropic motion of the ethylbenzene guest is impossible. Judging from the cavity structure, it is reasonable that the azimuth  $\Phi_1$  has a small constant value around  $10^\circ$  through the whole observed temperature region. In the case of a free ethylbenzene molecule, the activation energy for the rotation of the ethyl group is estimated to be 5.4–7.7 kJ/mol.<sup>10</sup> Therefore, fast free rotation of the ethyl group takes place easily even at 130 K, if there is no structural barrier around the ethyl group. However, in this case the azimuth  $\Phi_2$  has restriction coming from the cavity structure, so that the increase of  $\Phi_2$  in higher temperature region is limited to a small range of  $31.0^\circ$ – $36.8^\circ$ .

Above 290 K, the spectra of the  $\text{C}_6\text{H}_5\text{CD}_2\text{CH}_3$  clathrate changed their shapes and lost their intensity as shown in Figure 8g–k. A change of the motional mode of the ethyl group is expected. At 433 K, the observed spectrum Figure 8l showed an overlapped pattern of two axial line shapes. The wider axial pattern comes from the methylene part and the narrower axial pattern comes from the methyl part of the impurities. These axial shapes indicate that the ethyl group is in a rotational motion. For this motion, we considered Motion-E3 as shown in Figure 10d: the ethyl group is undergoing precessional rotation about an axis (the  $z$  axis in Figure 10d) which is inclined from the molecular geometrical principal axis (dashed line) by

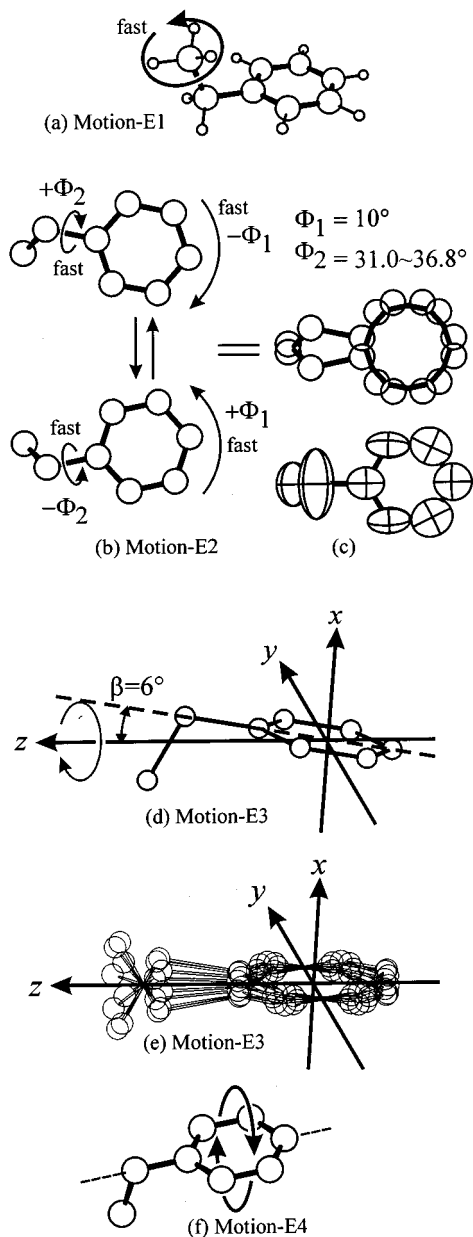


**Figure 10.** (a) Motion-E1. A fast rotational motion of the methyl part of an ethylbenzene molecule. Actual modeling is the same as that of Model-T1. (b) Motion-E2. An in-plane two-site reorientational motion combined with a two-site reorientation of the whole ethylbenzene ( $\pm\Phi_1$ ) and a two-site reorientation of the ethyl group ( $\pm\Phi_2$ ). The jump takes place between the site with  $-\Phi_1$  and  $+\Phi_2$  and the site with  $+\Phi_1$  and  $-\Phi_2$ . (c) Molecular structure of the ethylbenzene guest determined by X-ray diffraction method at room temperature.<sup>7</sup> (d) Motion-E3. A motional model for the ethylbenzene guest at 433 K. The ethyl part is undergoing a precessional motion about the  $z$  axis. The aromatic ring is undergoing a librational motion where the aromatic ring is almost maintained on the  $yz$  plane (see text). (e) Trajectory of the ethylbenzene molecule in Motion-E3. (f) Motion-E4. A  $180^\circ$  flip motion of the aromatic ring. Actual modeling is the same as that of Model-T2.

$\beta$ , but the aromatic part is undergoing librational motion in which the aromatic ring is almost maintained on the  $yz$  plane. The value for  $\beta$  was determined to be  $6^\circ$  from line-shape simulation. The  $z$  axis is very close to the principal axis for the least moment of inertia, whose  $\beta$  is  $8.3^\circ$ . The librational motion of the aromatic ring is modeled by the Euler angle setting of  $\alpha = 0 \sim 360^\circ$ ,  $\beta = 6^\circ$ , and  $\gamma = -\alpha$ . The trajectory of the guest ethylbenzene in Motion-E3 is illustrated in Figure 10e. The simulated pattern based on Motion-E3 is shown in Figure 8s.

The structural conditions around the guest ethylbenzene are very similar to those of the toluene clathrate. It is obvious that much space around the guest is necessary for Motion-E3. As shown in Figure 4, the TG curve of the ethylbenzene clathrate is very similar to that of the toluene clathrate. In the case of the ethylbenzene clathrate, ca. 60% of the guest is released in the temperature range between 350 and 450 K; and the sample that was once heated to 433 K showed a line shape very similar to that at 433 K even at 323 K. Therefore, the change from Motion-E2 to Motion-E3 takes place accompanied by the release of the guest, and Motion-E3 is possible in the space generated by the release of the guest.

The observed patterns (Figure 9a–k) of the C<sub>6</sub>D<sub>5</sub>CH<sub>2</sub>CH<sub>3</sub> clathrate were very similar to those of the toluene clathrate, though the pattern coming from the methyl group of the impurities was attached on them. The crystal structure of the ethylbenzene clathrate including the position of the guest molecule is very similar to the toluene clathrate. Therefore, the  $180^\circ$  flip motion of the aromatic ring of the ethylbenzene guest is very considerable. This  $180^\circ$  flip motion is modeled as Motion-E4 in Figure 10f. The simulated patterns based on Motion-E1, Motion-E2, and Motion-E4 are shown in Figure 9l–r. The correspondence between the observed and the simulated patterns are good. The activation energy calculated on the assumption of the Arrhenius relation was 36(4) kJ/mol, which is close to the value of the toluene clathrate. This means that the structural situations around the aromatic ring for both clathrates are very similar. Figure 9s is a simulated pattern at 433 K, in which Motion-E1, Motion-E3, and Motion-E4 are involved.

In conclusion, we have presented some images of the motional behavior of the benzene, toluene, and ethylbenzene guest of the [N(CH<sub>3</sub>)<sub>4</sub>][Cd<sub>3</sub>(CN)<sub>7</sub>] type clathrate before and during its thermal decomposition. The images show the process that the guest molecules are getting their motional amplitude more and more with an increase in temperature. These images have been constructed with several simple motional models, and they satisfy the results of the <sup>2</sup>H NMR powder pattern measurements and the X-ray crystallography. The simple motions used here are the in-plane rotational motion of a benzene ring, the rotational motion of a methyl group, the reorientational and the rotational motion of an ethyl group, the  $180^\circ$  flip motion of an aromatic ring, the precessional motion, and their modified motions. They are fundamental motions for this type of guest molecules. Perhaps it is difficult and unrealistic to apply these models to other cases directly, because the structural situations around guests are different case by case. However, the fundamental motions and the way of constructing a more complex motion presented here may be a guide for considering other guest molecular motions.

Many preparative and structural studies have clarified that the polycyano-polycadmate host system has many possibilities to form various types of host structures. A next step is to use the system for preparing new materials having some chemical or physical properties. In such step, the design of a host that includes functional guests and arrays them in its cavity will be necessary. At that time, we must take care of the fact that the guest that is arrayed definitely from the standpoint of the X-ray crystallography has a possibility of undergoing a reorientational motion more vigorous than we expect. Along the above line, recently we have prepared some new polycyano-polycadmate clathrates that show a response to UV and visible light. We consider that the orientation of the guest in the cavity, and the guest–guest and the guest–host interaction, are important for

the appearance of their interesting property. The information and experience obtained here will be useful in the analysis of the property. Its detailed study is now in progress and will be reported elsewhere.

**Acknowledgment.** This work was supported by a Grant-in-Aid for Scientific Research (C) Project No. 09640596 from the Ministry of Education, Science, Sports and Culture of Japan.

## References and Notes

- (1) (a) Iwamoto, T. In *Inclusion Compounds*; Atwood, J. L., Davies, J. E. D., MacNicol, D. D., Eds.; Academic Press: New York, 1984; Vol. 1, p 29. (b) Iwamoto, T. In *Inclusion Compounds*; Atwood, J. L., Davies, J. E. D., MacNicol, D. D., Eds. Oxford University Press: London, 1991; Vol. 5, p 177.
- (2) (a) Kitazawa, T.; Nishikiori, S.; Kuroda, R.; Iwamoto, T. *Chem. Lett.* **1988**, 459. (b) Kitazawa, T.; Nishikiori, S.; Kuroda, R.; Iwamoto, T. *Chem. Lett.* **1988**, 1729.
- (3) (a) Abrahams, B. F.; Hoskins, B. F.; Robson, R. *J. Chem. Soc., Chem. Commun.* **1990**, 60. (b) Hoskins, B. F.; Robson, R. *J. Am. Chem. Soc.* **1990**, *112*, 1546. (c) Abrahams, B. F.; Hoskins, B. F.; Liu, J.; Robson, R. *J. Am. Chem. Soc.* **1991**, *113*, 3045. (d) Abrahams, B. F.; Hardie, M. J.; Hoskins, B. F.; Robson, R.; Williams, G. A. *J. Am. Chem. Soc.* **1992**, *114*, 10641. (e) Nishikiori, S.; Ratcliffe, C. I.; Ripmeester, J. A. *J. Am. Chem. Soc.* **1992**, *114*, 8590. (f) Kitazawa, T.; Sugisawa, H.; Takeda, M.; Iwamoto, T. *J. Chem. Soc., Chem. Commun.* **1993**, 233. (g) Kim, J.; Whang, D.; Lee, J. I.; Kim, K. *J. Chem. Soc., Chem. Commun.* **1993**, 1400. (h) Kim, J.; Whang, D.; Koh, Y.-S.; Kim, K. *J. Chem. Soc., Chem. Commun.* **1994**, 637. (i) Abrahams, B. F.; Hardie, M. J.; Hoskins, B. F.; Robson, R.; Sutherland, E. E. *J. Chem. Soc., Chem. Commun.* **1994**, 1049. (j) Pickardt, J.; Gong, G.-T. *Z. Anorg. Allg. Chem.* **1994**, *620*, 183. (k) Kitazawa, T.; Nishikiori, S.; Kuroda, R.; Iwamoto, T. *J. Chem. Soc., Dalton Trans.* **1994**, 1029. (l) Kitazawa, T.; Kikuyama, T.; Takahashi, M.; Takeda, M. *J. Chem. Soc., Dalton Trans.* **1994**, 2933. (m) Ruiz, E.; Alvarez, S. *Inorg. Chem.* **1995**, *34*, 5845. (n) Kitazawa, T.; Kikuyama, T.; Takeda, M.; Iwamoto, T. *J. Chem. Soc., Dalton Trans.* **1995**, 3715. (o) Iwamoto, T. In *Comprehensive Supramolecular Chemistry*; MacNicol, D. D., Toda, F., Bishop, R., Eds.; Pergamon: New York, 1996; Vol. 6, p 644. (p) Kitazawa, T. *J. Inclusion Phenom.* **1996**, *26*, 153. (q) Kitazawa, T. *Mol. Cryst. Liq. Cryst.* **1996**, *276*, 167. (r) Kitazawa, T.; Kikuyama, T.; Ugajin, H.; Takahashi, M.; Takeda, M. *J. Coord. Chem.* **1996**, *37*, 17. (s) Kim, J.; Kim, K. *J. Coord. Chem.* **1996**, *37*, 7. (t) Kim, C.-H.; Soma, T.; Nishikiori, S.; Iwamoto, T. *Chem. Lett.* **1996**, 89. (u) Iwamoto, T. *J. Inclusion Phenom.* **1996**, *24*, 61. (v) Kurihara, H.; Nishikiori, S.; Iwamoto, T. *Chem. Lett.* **1997**, 61. (w) Iwamoto, T.; Nishikiori, S.; Kitazawa, T.; Yuge, H. *J. Chem. Soc., Dalton Trans.* **1997**, 4127. (x) Kitazawa, T. *J. Mater. Chem.* **1998**, *8*, 671. (y) Kitazawa, T. *Chem. Commun.* **1999**, 891.
- (4) (a) Nishikiori, S.; Ratcliffe, C. I.; Ripmeester, J. A. *J. Phys. Chem.* **1990**, *94*, 8098. (b) Nishikiori, S.; Ratcliffe, C. I.; Ripmeester, J. A. *J. Phys. Chem.* **1991**, *95*, 1589. (c) Nishikiori, S.; Ratcliffe, C. I.; Ripmeester, J. A. *Can. J. Chem.* **1993**, *71*, 1810.
- (5) (a) Nishikiori, S.; Soma, T.; Iwamoto, T. *J. Inclusion Phenom.* **1997**, *27*, 233. (b) Nishikiori, S. *J. Inclusion Phenom.* **1999**, *34*, 331.
- (6) Kitazawa, T.; Nishikiori, S.; Iwamoto, T. *J. Chem. Soc., Dalton Trans.* **1994**, 3695.
- (7) (a) Kim, C.-H.; Nishikiori, S.; Iwamoto, T. *Chem. Lett.* **1995**, 409. (b) Kim, C.-H.; Nishikiori, S.; Iwamoto, T. *Mol. Cryst. Liq. Cryst.* **1996**, *276*, 13.
- (8) (a) Solomon, I. *Phys. Rev.* **1958**, *110*, 61. (b) Davis, J. H.; Jeffrey, K. R.; Bloom, M.; Valic, M. I.; Higgs, T. P. *Chem. Phys. Lett.* **1976**, *42*, 390.
- (9) (a) Spiess, H. W.; Sillescu, H. *J. Magn. Reson.* **1981**, *42*, 381. (b) Vega, A. J.; Luz, Z. *J. Chem. Phys.* **1987**, *86*, 1803. (c) Greenfield, M. S.; Ronemus, A. D.; Vold, R. L.; Vold, R. R.; Ellis, P. D.; Raidy, T. E. *J. Magn. Reson.* **1987**, *72*, 89. (d) Wittebort, R. J.; Olejniczak, E. T.; Griffin, R. G. *J. Chem. Phys.* **1987**, *86*, 5411.
- (10) (a) Farkas, Ö.; Salpietro, S. J.; Császár, d, P.; Csizmadia, I. G. *J. Mol. Struct. (THEOCHEM)* **1996**, *367*, 25. (b) Benassi, R.; Taddei, F. *J. Mol. Struct. (THEOCHEM)* **1997**, *418*, 59, and references therein.